Published in final edited form as:
Biosens Bioelectron. 2006 March 15; 21(9): 1804–1811. doi:10.1016/j.bios.2005.09.008.

Toxin detection based on action potential shape analysis using a realistic mathematical model of differentiated NG108-15 cells

Dinesh K Mohan[2], **Peter Molnar**[1,2], and **James J. Hickman**[1,2,*]

[1]Nanoscience Technology Center, University of Central Florida, Orlando, FL 32826

[2]Department of Electrical Engineering, Clemson University, Clemson, SC 29634, U.S.A

Abstract

The NG108-15 neuroblastoma / glioma hybrid cell line has been frequently used for toxin detection, pharmaceutical screening and as a whole-cell biosensor. However, detailed analysis of its action potentials during toxin or drug administration has not been accomplished previously using patch clamp electrophysiology. In order to explore the possibility of identifying toxins based on their effect on the shape of intracellularly or extracellularly detected action potentials, we created a computer model of the action potential generation of this cell type. To generate the experimental data to validate the model, voltage dependent sodium, potassium and high-threshold calcium currents, as well as action potentials, were recorded from NG108-15 cells with conventional whole-cell patch-clamp methods. Based on the classic Hodgkin-Huxley formalism and the linear thermodynamic description of the rate constants, ion-channel parameters were estimated using an automatic fitting method. Utilizing the established parameters, action potentials were generated in the model and were optimized to represent the actual recorded action potentials to establish baseline conditions. To demonstrate the applicability of the method for toxin detection and discrimination, the effect of tetrodotoxin (a sodium channel blocker) and tefluthrin (a pyrethroid that is a sodium channel opener) were studied. The two toxins affected the shape of the action potentials differently and their respective effects were identified based on the changes in the fitted parameters. Our results represent one of the first steps to establish a complex model of NG108-15 cells for quantitative toxin detection based on action potential shape analysis of the experimental results.

Keywords

Action potential shape analysis; Toxin detection; NG108-15; Computer simulation; Linear the rmodynamic model; Hodgkin-Huxley model

1. Introduction

In the areas of environmental protection, toxicology and drug development there are increasing demands for high-throughput functional screening methods (Rogers 1995; Paddle 1996; Ohlstein, Ruffolo et al. 2000; Heck, Roy et al. 2001; Croston 2002; Tzoris, Fearnside et al. 2002). For monitoring of the environment, whole-cell biosensors could be more effective than physico-chemical methods to assess the global toxicity of the wide variety of chemicals that are possible pollutants (Evans, Briers et al. 1986; Rogers 1995; Bousse 1996; Paddle 1996; Naessens and Tran-Minh 1998). Whole-cell biosensors are also able to give functional information about the effect of chemicals, have the ability to detect unknown compounds and

*Corresponding Author Address: 12424 Research Parkway, Suite 400, Orlando, FL 32826, Phone: (864) 710 8472, Fax: (407 882 1156, jhickman@mail.ucf.edu.

continuous monitoring of external conditions is possible as they can be made small enough to allow field applications (Bousse 1996). Another benefit of whole cells in environmental applications is that they allow the measurement of the total bioavailability of a given pollutant rather than its free form (Bousse 1996; Naessens and Tran-Minh 1998; Philp, Balmand et al. 2003). Similarly, in safety pharmacology, the side effect spectrum of a given compound is not known, thus, the application of complex functional tests at the whole-organism-level are necessary (Jorkasky 1998;Kinter and Valentin 2002) and could be addressed with this technique. Moreover, the availability of genomic information significantly increased the number of potential targets available for drug discovery and new methods are necessary for high-throughput functional screening for target validation (Ohlstein, Ruffolo et al. 2000; Croston 2002).

Recently, the application of whole-cell biosensors for toxin detection and drug screening has become more readily accepted (Bousse 1996; Bentleya, Atkinsona et al. 2001; Baeumner 2003) as it has many benefits compared to traditional methods of evaluation. Several techniques have been developed to quantify the physiological changes induced by chemicals in whole-cell biosensors (Bousse 1996; Bentleya, Atkinsona et al. 2001). One of these techniques, which is frequently used for monitoring the physiological state / activity of excitable cells, is multi-electrode extracellular recording of membrane potential (Bousse 1996; Gross, Harsch et al. 1997; Denyer, Riehle et al. 1998; Jung, Cuttino et al. 1998; Offenhausser and Knoll 2001; Krause, Ingebrandt et al. 2000; Stett, Egert et al. 2003). The high-throughput or long-term application of extracellular recording is much preferred over intracellular action potential recording for many applications because the use of an intra-cellular or patch clamp electrode limits the life of the cell to a few hours as does the use of voltage sensitive dyes (all dyes reported to date, to a greater or lesser extent, are toxic to cells) (Mason 1993; Chiappalone, Vato et al. 2003).

Action potential generation and the shape of the action potential depends on the status of several ion channels located in a cell's membrane, which are regulated by receptors and intracellular messenger systems (Gross, Rhoades et al. 1995; Gross, Harsch et al. 1997; Morefield, Keefer et al. 2000). Changes in the extracellular (receptor activation) or intracellular environment (gene expression), in many cases, can be reflected in an alteration of spontaneous firing properties such as the frequency and firing pattern (Gross, Harsch et al. 1997; Amigo, Szczepanski et al. 2003; Chiappalone, Vato et al. 2003; Xia, Gopal et al. 2003) of excitable cells and also in changes in the shape of their action potentials (Clark, Bouchard et al. 1993; Muraki, Imaizumi et al. 1994; Akay, Mazza et al. 1998; Nygren, Fiset et al. 1998; Djouhri and Lawson 1999). There are many examples indicating that the shape of action potential depends on the extracellular and intracellular environment of the cells. Sodium (Spencer, Yuill et al. 2001), potassium (Clark, Bouchard et al. 1993; Martin-Caraballo and Greer 2000) and calcium channel modulators (Ahmed, Hopkins et al. 1993; van Soest and Kits 1998), as well as several toxins and various pathological conditions (Muraki, Imaizumi et al. 1994; Shaw and Rudy 1997; Akay, Mazza et al. 1998; Djouhri and Lawson 1999) have already been shown to affect the shape of action potentials. However, action potential shape analysis for high-throughput screening applications, such as toxin detection or drug screening, has not yet been developed. Two primary reasons this type of analysis has been lacking to date is that it is difficult to obtain high fidelity recordings from chip-based extracellular electrodes and from the lack of models to adequately analyze the signals.

Several mathematical models have been developed to describe the electrical properties and the process of action potential generation in excitable cells (Agin 1972; Cohen 1976; Otten 1995; Dokos 1996; Weiss 1996; Shevtsova 2003). The most widely used is the Hodgkin-Huxley formalism where ion channel activation and inactivation is described using voltage dependent activation and inactivation gates (Weiss 1996). In the original model the voltage

and time dependence of the gates was given utilizing rate constants, which were taken as an empirical function of the membrane potential (Hodgkin.L.A and Huxley.F.A 1952). However, in lieu of using empirical functions, it is also possible to deduce the functional form of the voltage dependence of the rate constants from thermodynamics (Weiss 1996; Destexhe and Huguenard 2000). The applications of these models to extracellular recordings from a suitable excitable cell population, in combination with the proper models, would be a logical next step in adapting this technology to high throughput toxin detection and drug discovery.

The NG108-15 hybrid cell line, which was created by merging mouse neuroblastoma and rat glioma cells, has been widely used in *in vitro* experiments as a substitute for primary-cultured neurons (Hu, Huang et al. 1997; Doebler 2000; Tojima, Yamane et al. 2000). The neuronal functions and features of differentiated NG108-15 cells have been well characterized, e.g. the presence of a wide range of voltage dependent and transmitter activated membrane currents have been detected as well as second messengers and enzymes normally found in primary neurons (Schmitt and Meves 1995; Lukyanetz 1998; Ma, Pancrazio et al. 1998; Tojima, Yamane et al. 2000). NG108-15 cells are widely used in pharmacology (Hu, Huang et al. 1997) and also as a whole-cell biosensor for toxin detection (Ma, Pancrazio et al. 1998). One of the distinctive features of the NG108-15 cell line, which makes it ideal for whole-cell biosensor applications, is that the cells do not form synaptic connections, thus network activity does not influence single cell data (Ma, Grant et al. 1999).

In this study we created a computer model of the action potential generation of an NG108-15 cell based on voltage-clamp and current clamp electrophysiological recordings. Using this model we developed and demonstrated the applicability of action potential shape analysis as a method for toxin detection and monitoring the physiological state of excitable cells.

2. Methods

2.1. Surface chemistry

NG108-15 cells were plated on N-1[3-(trimethoxysilyl) propyl]diethylenetriamine (DETA) coated glass coverslips (22×22mm, Thomas Scientific). The DETA coated coverslips were prepared according to published protocols (Schaffner, Barker et al. 1995). In brief, glass coverslips were cleaned using HCl/methanol (1:1) followed by a concentrated H_2SO_4 soak for 30 min followed by a water rinse. The coverslips were then boiled in deionized water followed by a rinse with acetone and then oven dried. The DETA films were formed by the reaction of the cleaned surfaces with a 0.1% (v/v) mixture of the organosilane in toluene. The DETA cover glasses were heated to just below the boiling point of toluene, rinsed with toluene; reheated to just below the boiling temperature again and then oven dried.

2.2. Culture of NG108-15 cells

The NG108-15 cell line (passage number 16) was obtained from Dr. M. W. Nirenberg (NIH). The NG108-15 cells were cultured according to published protocols (Higashida, Streaty et al. 1986; Ma, Pancrazio et al. 1998). Briefly, the cell stock was grown in T-25 and T-75 flasks in 90% Dulbecco's modified Eagle's medium (DMEM, GIBCO) supplemented with 10% Fetal Bovine Serum and HAT supplement (GIBCO, 100x) at 37°C with 10% CO_2. Differentiation was induced by plating the cells in a serum-free defined medium (DMEM+N2 supplement, GIBCO) in 35mm culture dishes at a density of 40,000 cells/dish.

2.3. Electrophysiological recordings

Whole-cell patch clamp recordings were performed in a recording chamber on the stage of a Zeiss Axioscope 2 FS Plus upright microscope. The chamber was continuously perfused (2 ml/min) with the extracellular solution. The composition of the extracellular solution for the

recording of action potentials was (in mM): NaCl 140, KCl 3.5, $MgCl_2$ 2, $CaCl_2$ 2, Glucose 10, HEPES 10. For the recording of potassium currents 1 μM tetrodotoxin (TTX) was added to the extracellular solution. To minimize space-clamp errors, sodium currents were recorded in a 'decreased sodium' extracellular solution containing (in mM): NaCl 50, TEA-Cl 100, CsCl 5, $CaCl_2$ 1, $CoCl_2$ 1, $MgCl_2$ 1, Glucose 10, HEPES 10. For the recording of calcium currents, sodium and potassium channels were blocked with Cs, TEA and TTX. The extracellular solution composition for the measurement of calcium currents was (in mM): NaCl 100, TEA-Cl 30, $CaCl_2$ 10, $MgCl_2$ 2, Glucose 10, HEPES 10, TTX 0.001. The pH was adjusted to 7.3 and the osmolarity was 320 mOsm. The intracellular solutions composition for recording the action potentials and for potassium channel measurements was (in mM): Kgluconate 130, $MgCl_2$ 2, EGTA 1, HEPES 15, ATP 5, for sodium channels was CsF 130, NaCl 10, TEA-Cl 10, $MgCl_2$ 2, EGTA 1, HEPES 10, ATP 5 and for calcium channels was: CsCl 120, TEA-Cl 20, $MgCl_2$ 2, EGTA 1, HEPES 10, ATP 5 (pH = 7.2; osmolarity = 280 mOsm). For selecting L-type calcium channels, 1 μM ωCTxGVIA was used.

Patch pipettes (4–6 Mohm resistance) were prepared from borosilicate glass (BF150-86-10; Sutter, Novato, CA) with a Sutter P97 pipette puller. Voltage clamp and current clamp experiments were performed with a Multiclamp 700A (Axon, Union City, CA) amplifier. Signals were filtered at 2 kHz and digitized at 20 kHz with an Axon Digidata 1322A interface. Data recording and analysis was performed using pClamp 8 (Axon) software. Sodium and potassium currents were measured in voltage clamp mode using 10 mV voltage steps from a – 85 mV holding potential. To record high-threshold calcium currents, a – 40 mV holding was used. Whole cell capacitance and series resistance was compensated and a p/6 protocol was used. The access resistance was less than 22 Mohm. Action potentials were measured in current-clamp mode using 1 s depolarizing current injections. Data was saved in text-format and imported into MATLAB for further analysis.

2.4. Simulation of ionic conductance's and action potential generation in NG108-15 cells

The classic Hodgkin-Huxley model (Hodgkin and Huxley 1952) was used for the description of the ion channel currents, but instead of the original empirical description of the rate constant, the thermodynamic approach (Weiss, Urbaszek et al. 1995; Destexhe and Huguenard 2000) was applied. Briefly, the total ionic membrane current was described as:

$$I_{ionic}=I_{Na}+I_K+I_{Ca}+I_l=\bar{g}_{Na}m^3h(V-V_{Na})+\bar{g}_K n^4(V-V_K)+\bar{g}_{CaL}e^3(V-V_{CaL})+\bar{g}_l(V-V_l)$$

Dynamic changes in the membrane-potential were calculated according to:

$$\frac{dV}{dt}=\frac{I_{external}-I_{ionic}}{C_M}$$

The dynamics of the state variables was given as $\frac{dm}{dt}=\frac{m_\infty-m}{\tau_m}$. Where $\bar{g}_{Na}$, $\bar{g}_K$, $\bar{g}_{CaL}$, V_{Na}, V_K, V_{CaL} are constants; m, n, h, e are the state variables, m_∞, n_∞, h_∞, e_∞ are the steady-state values of the state variables and the τ-s are their voltage-dependent time-constants. The voltage-dependence of the steady-state state parameters and the time constants were given using the general thermodynamic formalism:

$$m_\infty=\frac{1}{1+\exp^{-\frac{zF}{RT}(V_m-V_{\frac{1}{2}})}}\text{ and }\tau_m=\frac{A}{\exp^{\frac{zF}{RT}\xi(V_m-V_{\frac{1}{2}})}\cosh(\frac{zF}{2RT}(V_m-V_{\frac{1}{2}}))}$$

Where z,$V_{½}$, A and ξ are fitting parameters and V_m represents the membrane potential. As it can be seen from these equations $V_{½}$ corresponds to the half activation/inactivation potential of the channel and A is linearly related to the activation or inactivation time-constant. The meanings of z and ξ are not as obvious: z is related to the number of moving charges during the opening or closing of the channel; whereas ξ describes the asymmetric position of the moving charge in the cell membrane. Sodium, potassium and calcium channel mediated currents, which were recorded in voltage-clamp mode at different membrane potentials (10 mV increments, −40 mV, +30 mV range), were fitted in one step using the above described model, with the corresponding ion channels included, using the built-in routines (fminunc) of MATLAB through a custom-made graphical interface. Parameters obtained from different cells were averaged (n = 4–6) and considered as initial values for the action potential modeling. Simulated action potentials were fitted to the experimental data using built-in functions in MATLAB (fminunc). Fminunc is used to find a minimum of a scalar function (the error function, see in Results) of several variables, starting at an initial estimate. This method is generally referred to as unconstrained nonlinear optimization. Because it is finding only local minimums, it is very important to start the optimization as close to the final result as it is possible. In our case, the averaged ion channel parameters obtained from voltage clamp experiments served the initial values for the parameter estimations.

3. Results

The NG108-15 cells completed their differentiation process and a neuronal phenotype was obtained by day 10 *in vitro* (DIV) in the defined, serum-free medium (Figure 1A). Electrophysiological experiments were performed on the differentiated cells between day 10 and 14 *in vitro*. All of the cells investigated showed pronounced sodium, potassium and calcium currents in the voltage-clamp experiments. Most of the cells fired one single action potential upon depolarization in current-clamp mode, whereas about 10% of the cells were able to fire multiple action potentials. Only a very small minority of the cells (about 5%) were spontaneously active.

3.1. Extracting ion-channel parameters from the voltage-clamp experiments using the linear thermodynamic description

Signals from sodium, potassium and high-threshold (L-type) calcium channels were recorded in voltage-clamp mode using the Axon's pClamp 8 program with standard protocols (Figure 1B, C). The data were saved in ASCII format and imported into the MATLAB program. A graphical interface was created to fit the mathematical model to the experimental data and to visualize the results. To quantify the difference between the fitted curves and the recorded data the following error-functions were implemented:

1. Maximum error: $E_{Max} = Max(Abs(R(t_n) - S(t_n)))$ where $R(t_n)$ is the recorded value and $S(t_n)$ is the simulated data at time t_n.
2. Least Square: $E_{Lsquare} = \Sigma_n (R(t_n) S(t_n))^2$.
3. Weighted Least Square: $E_{WLsquare} = E_{Lsquare}$ if $t_n<30$ ms and $E_{WLsquare} = 5 *E_{Lsquare}$ if $t_n \geq 30$ ms.

After several trials it was concluded that simulations using the Weighted Least Square Error function gave the most satisfactory results because the other Error Functions occasionally obtained a non-inactivating sodium-current component in the simulated data. Curves were fitted after an initial 0.1 ms delay to eliminate the effect of experimental artifacts. In some simulations the reversal potential for the ionic conductances was kept constant.

In general, an excellent fit to the potassium channel data (Figure 1B, C) and an acceptable fit to the sodium and calcium channel data was achieved. The automatic fitting algorithm converged in less than 2 min. running on a Pentium III 1GHz personal computer. After averaging the results of 3–10 experiments the initial parameter values for modeling the action potentials were obtained (Table 1).

3.2. Action potential shape analysis

Action potentials were evoked with short (2 ms) current injections in current clamp mode either at resting membrane potential or at a – 85 mV holding potential. The following parameters were obtained from the patch-clamp recordings and used in the modeling: membrane resistance, resting membrane potential, membrane capacitance and injected current. The maximum conductance of the leakage current ($\mathbf{g_l}$) was calculated from the ionic conductances and from the resting membrane potential. We used the earlier established, averaged ion-channel parameters as the initial parameters for the action potential fitting. Using voltage dependent sodium, potassium and L-type calcium conductances, an excellent fit to the rising and to the initial falling phase of the action potentials in the NG108-15 cells was obtained (Figure 2).

We also obtained an excellent fit to the experimental data in the case of the toxin-modified action potentials by modifying only the corresponding sodium-channel parameters (Figure 2, Table 2).

4. Discussion

We have developed a mathematical model of the action potential generation in NG108-15 cells and extracted the parameters for this model from whole-cell patch clamp experiments. Utilizing only voltage-sensitive sodium, potassium and L-type calcium channels we were able to obtain an excellent fit to the rising as well as to the initial falling phase of the action potential. The weak fit to the later falling phase of the action potential could be due to active conductances which were not taken into account in this model. For example, at lease three other calcium channels and also a calcium activated potassium channel have already been described in NG108-15 cells. In this study we kept the number of the ion channels modeled to a minimum, due to the high computational requirements of the parameter fitting program.

A linear thermodynamic formalism was used to describe the voltage and time dependence of the ionic conductances, which eliminated the need for ‘guessing’ the function for the voltage-dependence of the rate constants and the same form (with different parameters) could be used for the characterization of all the ion channels.

One of the limitations of the model is the high number of parameters required to describe the ionic conductances. In this study 4 parameters were used to characterize each activation/inactivation gate, thus, for the description of the sodium channel, a total of 10 parameters was required. With this high number of parameters a more detailed study is needed to prove the uniqueness and stability of the solutions.

In order to validate the action potential shape analysis for utilization as a toxin detection method, the effect of two toxins, tetrodotoxin, a specific sodium channel blocker, and tefluthrin, a sodium channel opener pyrethroid were analyzed. Changes in the action potential shape, and also in the fitted ion-channel parameters caused by the two toxins, were measured. An excellent fit to the toxin-modified action potential shapes by modifying only the appropriate sodium channel parameters has been achieved. TTX, as expected from a channel blocker, significantly decreased the maximum sodium conductance, but did not affect the voltage dependence of the channel (Table 2.). Unexpectedly, TTX affected the activation kinetics of the sodium channels as well. TTX moderately increased the activation **A** parameter by causing a slowing down of

the activation of the channel. One possible explanation could be the existence of different subpopulations of sodium channels on the NG108-15 cells with different activation and inactivation time constants and different TTX sensitivities.

The major effect of tefluthrin (a channel opener) was to slow down (practically remove) the inactivation of the sodium channels. Tefluthrin also affected the maximum sodium channel conductance and the voltage dependence of the activation and inactivation of the channel, shifting appropriate current-voltage (I/V) relationships to the left by about 15 mV. A Similar effect on the voltage dependence of the sodium channels was described by Spencer et al. (2001) for fenpropathrin, a tefluthrin-like pyrethroid.

In summary, these experiments indicated that we were able to decipher and quantify the effects of toxins on ion channels without actually measuring ion channel currents in voltage-clamp experiments. Instead, changes in the shape of action potentials measured by patch clamp electrophysiology, combined with a validated computer simulation of the cell, were utilized.

This method could be useful for toxin detection and for classification of unknown toxins in environmental protection scenarios or in the detection of biological and chemical warfare agents. It could also be extended to functional screening in drug development. With the refinement of the model of the cell not only those toxins could be identified, which are directly acting on ion channels, but also changes in second messenger levels or gene expression could also be detected and classified. Moreover, recent advancements in the study of the cell electrode interface and microelectrode-fabrication technology indicate that high-fidelity extracellular recording of action potential shapes might be possible, which opens a new horizon for the high-throughput application of our method using extracellular recordings.

4. Conclusions

We have demonstrated that toxin effects on ionic membrane currents can be quantified based on the measurement of changes in action potential shape and a realistic mathematical model of action potential generation in NG108-15 cells. Further studies are underway to improve the mathematical model, explore the applicability of the method for detection and identification of a wider variety of toxins and to extend the technique to enable obtaining high-fidelity action potential data with non-invasive, high-throughput extracellular electrodes, in order to make high-throughput functional toxin detection and drug screening possible.

Acknowledgments

The Hunter endowment at Clemson University and DOE grant number DE-FG02-00ER45856 for funding the study; Dr. M. W. Nirenberg (NIH) for kindly supplying the NG108-15 cell line. Initial experiments were done at Clemson University as indicated by the dual affiliations of Drs. Molnar and Hickman.

References

Agin, D. Excitability phenomena in membranes. In: Rosen, R., editor. Foundations of Mathematical Biology. New York: Academic Press; 1972. p. 253-277.

Ahmed IA, Hopkins PM, et al. Caffeine and Ryanodine Differentially Modify a Calcium- Dependent Component of Soma Action-Potentials in Identified Molluscan (Lymnaea-Stagnalis) Neurons in-Situ. Comparative Biochemistry and Physiology C-Pharmacology Toxicology & Endocrinology 1993;105 (3):363–372.

Akay M, Mazza E, et al. Non-linear dynamic analysis of hypoxia-induced changes in action potential shape in neurons cultured from the rostral ventrolateral medulla (RVLM). Faseb Journal 1998;12(4): 2881.

Amigo JM, Szczepanski J, et al. On the number of states of the neuronal sources. Biosystems 2003;68 (1):57–66. [PubMed: 12543522]

Baeumner AJ. Biosensors for environmental pollutants and food contaminants. Analytical and Bioanalytical Chemistry 2003;377(3):434–445. [PubMed: 12920503]

Bentleya A, Atkinsona A, et al. Whole cell biosensors — electrochemical and optical approaches to ecotoxicity testing. Toxicology *in Vitro* 2001;15:469–475. [PubMed: 11566580]

Bousse L. Whole cell biosensors. Sensors and Actuators B-Chemical 1996;34(1–3):270–275.

Chiappalone M, Vato A, et al. Networks of neurons coupled to microelectrode arrays: a neuronal sensory system for pharmacological applications. Biosensors and Bioelectronics 2003;18:627–634. [PubMed: 12706572]

Clark RB, Bouchard RA, et al. Heterogeneity of Action-Potential Wave-Forms and Potassium Currents in Rat Ventricle. Cardiovascular Research 1993;27(10):1795–1799. [PubMed: 8275526]

Cohen, H. Mathematical developments in Hodgkin-Huxley theory and its approximations. In: Levin, SA., editor. Proceedings of the Ninth Symposium on Mathematical Biology held in New York, January, 1975; The American Mathematical Society; Washington. 1976. p. 89-124.

Croston GE. Functional cell-based uHTS in chemical genomic drug discovery. Trends in Biotechnology 2002;20(3):110–115. [PubMed: 11841862]

Denyer MCT, Riehle M, et al. Preliminary study on the suitability of a pharmacological bio- assay based on cardiac myocytes cultured over microfabricated microelectrode arrays. Medical & Biological Engineering & Computing 1998;36(5):638–644. [PubMed: 10367451]

Destexhe A, Huguenard JR. Nonlinear Thermodynamic Models of Voltage-Dependent Currents. Journal of Computational Neuroscience 2000;9:259–270. [PubMed: 11139042]

Djouhri L, Lawson SN. Changes in somatic action potential shape in guinea-pig nociceptive primary afferent neurones during inflammation *in vivo*. Journal of Physiology-London 1999;520(2):565–576.

Doebler JA. Effects of neutral ionophores on membrane electrical characteristics of NG108-15 cells. Toxicology Letters 2000;114(1–3):27–38. [PubMed: 10713466]

Dokos SC, B Lovell N. Ion Currents Underlying Sinoatrial Node Pacemaker Activity: A New Single Cell Mathematical Model. Journal of Theoretical Biology 1996;181(3):245–272. [PubMed: 8869126]

Evans GP, Briers MG, et al. Can Biosensors Help to Protect Drinking-Water. Biosensors 1986;2(5):287–300. [PubMed: 3619957]

Gross GW, Harsch A, et al. Odor, drug and toxin analysis with neuronal networks *in vitro*: Extracellular array recording of network responses. Biosensors & Bioelectronics 1997;12(5):373–393. [PubMed: 9228730]

Gross GW, Rhoades BK, et al. The Use of Neuronal Networks on Multielectrode Arrays as Biosensors. Biosensors & Bioelectronics 1995;10(6–7):553–567. [PubMed: 7612207]

Heck DE, Roy A, et al. Nucleic acid microarray technology for toxicology: Promise and practicalities. Biological Reactive Intermediates Vi 2001;500:709–714.

Higashida H, Streaty RA, et al. Bradykinin-Activated Transmembrane Signals Are Coupled Via No or Ni to Production of Inositol 1,4,5-Trisphosphate, a 2nd Messenger in Ng108-15 Neuroblastoma Glioma Hybrid-Cells. Proceedings of the National Academy of Sciences of the United States of America 1986;83(4):942–946. [PubMed: 3081891]

Hodgkin LA, Huxley FA. A quantitative description of membrane current and its application to conduction and excitation in nerve. Journal of Physiology 1952;117:500–544. [PubMed: 12991237]

Hu Q, Huang F, et al. Inhibition of Toosendanin on the delayed rectifier potassium current in neuroblastoma X glioma NG108-15 cells. Brain Research 1997;751:47–53. [PubMed: 9098567]

Jorkasky DK. What does the clinician want to know from the toxicologist? Toxicology Letters 1998;102–103:539–543.

Jung DR, Cuttino DS, et al. Cell-based sensor microelectrode array characterized by imaging x-ray photoelectron spectroscopy, scanning electron microscopy, impedance measurements, and extracellular recordings. Journal of Vacuum Science & Technology a-Vacuum Surfaces and Films 1998;16(3):1183–1188.

Kinter LB, Valentin JP. Safety pharmacology and risk assessment. Fundamental & Clinical Pharmacology 2002;16(3):175–182. [PubMed: 12165065]

Krause M, Ingebrandt S, et al. Extended gate electrode arrays for extracellular signal recordings. Sensors and Actuators B 2000;70:101–107.

Lukyanetz EA. Diversity and properties of calcium channel types in NG108-15 hybrid cells. Neuroscience 1998;87(1):265–274. [PubMed: 9722156]

Ma W, Grant GM, et al. Kir 4.1 channel expression in neuroblastoma×glioma hybrid NG108-15 cell line. Developmental Brain Research 1999;114(1):127–134. [PubMed: 10209250]

Ma W, Pancrazio JJ, et al. Neuronal and glial epitopes and transmitter-synthesizing enzymes appear in parallel with membrane excitability during neuroblastoma X glioma hybrid differentiation. Developmental Brain Research 1998;106:155–163. [PubMed: 9554993]

Martin-Caraballo M, Greer JJ. Development of potassium conductances in perinatal rat phrenic motoneurons. Journal of Neurophysiology 2000;83(6):3497–3508. [PubMed: 10848565]

Mason, TW. Fluorescent and Luminescent Probes for Biological Activity. London: Academic Press; 1993.

Morefield SI, Keefer EW, et al. Drug evaluations using neuronal networks cultured on microelectrode arrays. Biosensors & Bioelectronics 2000;15(7–8):383–396. [PubMed: 11219752]

Muraki K, Imaizumi Y, et al. Effects of Noradrenaline on Membrane Currents and Action- Potential Shape in Smooth-Muscle Cells from Guinea-Pig Ureter. Journal of Physiology-London 1994;481 (3):617–627.

Naessens M, Tran-Minh A. Whole-cell biosensor for determination of volatile organic compounds in the form of aerosols. Analytica Chimica Acta 1998;364(1–3):153–158.

Naessens M, Tran-Minh C. Whole-cell biosensor for direct determination of solvent vapours. Biosensors & Bioelectronics 1998;13(3–4):341–346.

Nygren A, Fiset C, et al. Mathematical model of an adult human atrial cell - The role of K+ currents in repolarization. Circulation Research 1998;82(1):63–81. [PubMed: 9440706]

Offenhausser A, Knoll W. Cell-transistor hybrid systems and their potential applications. Trends in Biotechnology 2001;19(2):62–66. [PubMed: 11164555]

Ohlstein EH, Ruffolo RR, et al. Drug discovery in the next millennium. Annual Review of Pharmacology and Toxicology 2000;40:177–191.

Otten EH, M Scheepstra K A. A model study on the influence of a slowly activating potassium conductance on repetitive firing patterns of muscle spindle primary endings. Journal of Theoretical Biology 1995;173(1):67–78. [PubMed: 7739213]

Paddle BM. Biosensors for chemical and biological agents of defence interest. Biosensors & Bioelectronics 1996;11(11):1079–1113. [PubMed: 8828162]

Philp JC, Balmand S, et al. Whole cell immobilised biosensors for toxicity assessment of a wastewater treatment plant treating phenolics-containing waste. Analytica Chimica Acta 2003;487:61–74.

Rogers KR. Biosensors for Environmental Applications. Biosensors & Bioelectronics 1995;10(6–7): 533–541.

Schaffner EA, Barker LJ, et al. Investigation of the factors necessary for growth of hippocampal neurons in a defined system. Journal of Neuroscience Methods 1995;62:111–119. [PubMed: 8750092]

Schmitt H, Meves H. Model experiments on squid axons and NG108-15 mouse neuroblastoma * rat glioma hybrid cells. Journal of Physiology (Paris) 1995;89:181–193.

Shaw RM, Rudy Y. Electrophysiologic effects of acute myocardial ischemia: a theoretical study of altered cell excitability and action potential duration. Cardiovascular Research 1997;35(2):256–272. [PubMed: 9349389]

Shevtsova NAP, K McCrimmon D, R Rybak IA. Computational modeling of bursting pacemaker neurons in the pre-Bötzinger complex. Neurocomputing 2003;52–54:933–942.

Spencer CI, Yuill KH, et al. Actions of Pyrethroid Insecticides on Sodium Currents, Action Potentials, and Contractile Rhytm in Isolated Mammalian Ventricular Myocytes and Perfused Hearts. The Journal of Pharmacology and Experimental Therapeutics 2001;298:1067–1082. [PubMed: 11504804]

Stett A, Egert U, et al. Biological application of microelectrode arrays in drug discovery and basic research. Analytical and Bioanalytical Chemistry 2003;377(3):486–495. [PubMed: 12923608]

Tojima T, Yamane Y, et al. Acquisition of neuronal proteins during differentiation of NG108-15 cells. Neuroscience Research 2000;37:153–161. [PubMed: 10867177]

Tzoris A, Fearnside D, et al. Direct toxicity assessment of wastewater: Baroxymeter, a portable rapid toxicity device and the industry perspective. Environmental Toxicology 2002;17(3):284–290. [PubMed: 12112637]

van Soest PF, Kits KS. Conopressin affects excitability, firing, and action potential shape through stimulation of transient and persistent inward currents in mulluscan neurons. Journal of Neurophysiology 1998;79(4):1619–1632. [PubMed: 9535933]

Weiss I, Urbaszek A, et al. Simulation of the Cardiac Action-Potentials of Various Cell- Types with Account Being Taken of Neural Influencing Factors. Biomedizinische Technik 1995;40(3):64–69. [PubMed: 7538801]

Weiss, TF. Cellular Biophysics. Cambridge, MA: The MIT Press; 1996.

Xia Y, Gopal KV, et al. Differential acute effects of fluoxetine on frontal and auditory cortex networks *in vitro*. Brain Research 2003;973(2):151–160. [PubMed: 12738058]

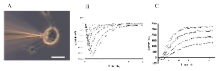

Figure 1.

Estimation of ion channel parameters from the voltage-clamp experiments. A: Phase-contrast picture of an NG108-15 cell with a patch-clamp electrode attached to the cell (40× objective, scale bar = 25 μm). B: Sodium currents recorded at different membrane potentials of −10, 0, 10, 20 mV in voltage-clamp mode (solid line) and the results of the parameter fitting using the Hodgkin-Huxley model and the linear thermodynamic formalism (dotted line). C: Potassium currents recorded at membrane potentials of 0, 10, 20 and 30 mV (solid line) and the fitted curves using the model (dotted line).

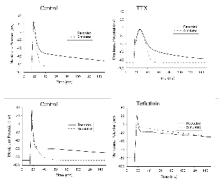

Figure 2.
Effect of toxins on the action potentials of NG108-15 cells. Upper panel: effect of 0.5 μM tetrodotoxin. Lower panel: effect of 0.5 μM tefluthrin. Solid line: data recorded in current clamp experiments. Dotted line: results of the simulation using the mathematical model of the NG108-15 cells.

Table 1

Average ion channel parameters characteristic of NG108-15 cells obtained by parameter fitting to voltage-clamp data (n = 3–10).

					Activation								Inactivation							
Channel	**g**	**SEM**	**V_{Rev}**	**SEM**	**z**	**SEM**	**$V_{1/2}$**	**SEM**	**ξ**	**SEM**	**A**	**SEM**	**z**	**SEM**	**$V_{1/2}$**	**SEM**	**ξ**	**SEM**	**A**	**SEM**
Sodium	343.59	183.23	72.35	6.31	5.98	0.30	−46.93	2.46	−0.38	0.01	0.58	0.12	−7.48	1.13	−64.36	4.73	0.41	0.01	1.31	0.17
Potassium	25.09	4.81	−80.00	0.00	2.78	0.46	−22.52	2.64	−0.26	0.02	2.12	0.16								
Calcium	7.45	1.88	32.00	0.00	3.15	0.96	−4.67	6.25	−0.30	0.37	0.84	0.37								
Leakage	5.22	0.89	−49.40	0.76																

Table 2

Effect of TTX and tefluthrin on the action potential parameters. Only sodium channel parameters are shown, the other ion-channel parameters did not change. Data shown as mean ± SEM. Bold: statistically significant ($p > 0.05$) change.

			Activation				Inactivation			
Na	**g**	**V_{Rev}**	**Z**	**$V_{1/2}$**	**ξ**	**A**	**z**	**$V_{1/2}$**	**ξ**	**A**
Contr	317±84	60	6±0.04	−6.9±0.3	−0.38±0.03	0.59±0.08	−7.5±0.04	−64±0.4	0.43±0.03	1.5±0.7
TTX	31±18	60	6±0.01	−6.9±0.3	−0.40±0.03	0.83±0.17	−7.5±0.1	−64±0.4	0.42±0.02	3.0±0.9
% Chg	**−89±6**	0	−0.6±0.6	0±0.004	5.9±5.2	**41±25.5**	0±0.002	0±0.001	−0.68±0.7	331±301
Contr	227±106	60	5.6±0.4	−46.7±0.2	−0.38±0	0.7±0.12	−7.4±0.1	−60±2.6	0.48±0.01	1.3±0.22
Tefl	44.6±11	60	5.6±0.4	−54±2.3	−0.36±0.02	1.5±0.6	−7.8±0.3	−69±2.1	0.47±0.04	39±18
% Chg	**−71±9**	0	1±1	**17±5**	−4±4.2	86±66	6±5.71	**15±2.2**	−2±7.9	**4410±2974**